Assessment of two non-invasive techniques for measuring turbulent benthic fluxes in a shallow lake

Felipe Breton, Guilherme Calabro-Souza, Andreas Lorke, Philippe Dubois, Magali Jodeau, Régis Moilleron, Brigitte Vinçon-Leite, Jiří Jan, Jakub Borovec, Bruno J. Lemaire

This article was published in *Environmental Pollution,* 2024, 124032
https://doi.org/10.1016/j.envpol.2024.124032

Assessment of two non-invasive techniques for measuring turbulent benthic fluxes in a shallow lake

Felipe Breton[a,b+]*, Guilherme Calabro Souza[c,d+], Andreas Lorke[e], Philippe Dubois[c], Magali Jodeau[d], Régis Moilleron[c], Brigitte Vinçon-Leite[c], Jiří Jan[a], Jakub Borovec[a ◘], and Bruno J. Lemaire[f, g ◘]

[a] ISBB, Biology Centre CAS, Ceske Budejovice, Czech Republic
[b] University of South Bohemia, Czech Republic.
[c] LEESU, Ecole des Ponts, Univ. Paris Est Creteil, Marne-La-Vallée, France
[d] LHSV, Ecole des Ponts, EDF R&D, Cerema, Chatou, France
[e] University of Kaiserslautern-Landau, Landau, Germany
[f] Université Paris-Saclay, INRAE, Hydrosystèmes Continentaux Anthropisés - Ressources, Risques, Restauration, Antony, France
[g] Université Paris-Saclay, AgroParisTech, Palaiseau, France

[+] These authors contributed equally to this work and share first authorship
◘ These authors share last authorship
* felipe.breton@bc.cas.cz

Abstract

Benthic fluxes refer to the exchange rates of nutrients and other compounds between the water column and the sediment bed in aquatic ecosystems. Their quantification contributes to our understanding of aquatic ecosystem functioning. Near-bed hydrodynamics plays an important role at the sediment-water interface, especially in shallow lakes, but it is poorly considered by traditional measuring techniques of flux quantification, such as sediment incubations. Thus, alternative sampling techniques are needed to characterize key benthic fluxes under *in-situ* hydrodynamic conditions. This study aimed to evaluate the performance of two promising methods: relaxed eddy accumulation (REA) and mass transfer coefficient (MTC). We applied them in a hyper-eutrophic shallow lake to measure the fluxes of ammonium, phosphate, iron, and manganese ions. For the first time, REA revealed hourly nutrient flux variations, indicating a strong lake biogeochemical dynamics at short time-scales. Daily average fluxes are of similar orders of magnitude for REA and MTC for ammonium (24 and 42 mmol m^2 d^{-1}), manganese (1.0 and 0.8), and iron (0.8 and 0.7) ions. They are one order of magnitude higher than fluxes estimated from sediment incubations, due to the difficulty in reproducing *in-situ* oxygen and hydrodynamic conditions in the laboratory. Although the accuracy of both techniques needs to be improved, the results revealed their potential: REA follows the short-term biogeochemical dynamics of sediments, while MTC could be widely used for lake monitoring because of its simpler implementation.

Keywords: sediment-water interface; relaxed eddy accumulation; mass transfer coefficient; hydrodynamics; sediment; biogeochemistry

1. Introduction

Near-bed turbulence can influence benthic fluxes in aquatic ecosystems, i.e. the exchange rates of chemicals between the water column and the sediment bed (Boudreau and Jorgensen, 2001). These fluxes are mainly involved in primary production through nutrient recycling, the internal load (Søndergaard et al., 2003), but benthic fluxes of electron acceptors, gases, and pollutants are also relevant controls on water pollution (Jiang et al., 2022a) and sediment diagenesis (Emerson and Hedges, 2003; Sun et al., 2021). Hydrodynamic conditions can directly influence benthic fluxes: i) by mixing solutes in the water column, which affects the concentration gradient at the sediment-water interface (SWI) (Imboden and Wüest, 1995); ii) by modulating the thickness of the diffusive boundary layer (DBL) above low permeability sediments (Lorke et al., 2003); and iii) by resuspending sediments (Ding et al., 2017). Hydrodynamic conditions also indirectly influence benthic fluxes by modulating the influx of reactants and chemical reactions in sediment porewater (Santschi et al., 1990), beginning with the oxygen influx (Jiang et al., 2022b) and the phosphorus (P) release during organic matter decomposition (Gu et al., 2016; Jin et al., 2022). However, released P under oxic and suboxic conditions precipitates with iron and is immobilized on the sediment. Due to the close and complex coupling between solute transport processes and sediment biogeochemistry (Di Toro, 2001; Lerman, 1978; Paraska et al., 2014), the dynamics of fluxes expected for nutrients and metallic ions should differ from that of dissolved oxygen.

Hydrodynamic effects on benthic fluxes are particularly important in shallow lakes, where frequent wind-induced full-mixing episodes renew the water in contact with the sediment (Phillips, 2008). Under eutrophic conditions, the intense decay of organic matter creates sharp gradients of oxygen, nutrients, and alternative terminal electron-acceptors, such as iron and manganese, at the SWI. Many studies focused on the hydrodynamic control of benthic fluxes (Boudreau and Guinasso, 1981; Bryant et al., 2010; Cheng et al., 2014; Dade, 1993; Fan et al., 2010; Mackay et al., 2014), but it is still unclear under what range of current velocities and for which chemical compounds such control exists.

Techniques for quantifying benthic fluxes have been evolving (Coogan et al., 2022). Extensive reviews can be found in Viollier et al. (2003) and Boynton (2017). Traditional methods use sediment incubations, either *ex situ* with mixed sediments in flumes (e.g., Woodruff et al. 1999) or with undisturbed sediment cores (e.g., Seitaj et al. 2017), or *in situ* with benthic chambers (e.g., Kononets et al., 2021; Mustajärvi et al., 2017). Benthic fluxes are estimated either from concentration time-series measured in the overlying water or from concentration gradients measured at the SWI (Berg et al., 1998), detected by gel probes (Hesslein, 1976), or with electrochemical and optical microsensors (de Beer, 2011; Yamamoto et al., 2015). Their main limitations are their spatial and temporal resolution - typically a surface area of a few square centimetres that can be examined on a daily time-scale - and their ability to reproduce natural conditions, including hydrodynamics. Nevertheless, large efforts have been invested in designing stirred benthic chambers (Tengberg et al., 2005) and sediment incubations (Sulpis et al., 2019) that mimic natural conditions.

Concentration gradients and benthic fluxes can be measured directly in the natural environment by profilers or landers equipped with automatic microprofilers facilitating submillimetre resolution (e.g., Glud et al., 2021), or by gel probes for a wider range of solutes, but of coarser temporal and vertical resolution (e.g., Wang and Wang, 2017). The mass transfer coefficient method (MTC) (as explained in Thibodeaux et al. 2011) considers the concentration difference between the SWI and the turbulent boundary layer (TBL), rather than the interfacial gradient, which significantly simplifies sampling. This method takes hydrodynamics into account by a factor called the mass transfer coefficient or transfer velocity (Lorke and Peeters, 2006). Although it has been used by Grant et al. (2018) to estimate nitrogen fluxes in streams and by Koelmans et al. (2010) to estimate fluxes of hydrophobic organic chemicals in rivers, its application in shallow lakes is yet to be explored.

Another option is to track the turbulent fluctuations of both solute concentration and vertical velocity in the TBL above the sediment at high frequency. This is done by the aquatic eddy covariance (AEC) technique (Berg et al., 2003). Since it is restricted to fluxes of compounds that can be measured with fast-response sensors, such as oxygen, hydrogen ions (Long et al., 2015), hydrogen sulphide (McGinnis et al., 2011), and heat (Berg and Pace, 2017), a Relaxed Eddy Accumulation (REA) technique was developed to cover a broad range of benthic fluxes (Lemaire et al., 2017). This measurement principle was validated for oxygen fluxes by Calabro-Souza et al. (2023), but it remains to be assessed for measuring benthic fluxes of other compounds.

In summary, sampling techniques for *in-situ* measurements need to be able to characterize key benthic fluxes while considering the prevailing hydrodynamic conditions. This study investigates the potential of MTC and REA to quantify the fluxes of nutrients and metallic ions in a shallow lake by using sediment incubations and AEC as references.

2. Materials and methods

2.1. Aquatic eddy covariance

Aquatic eddy covariance (AEC) is a technique for measuring turbulent vertical fluxes. It neglects molecular diffusion and consumption or production processes below the measurement height, and assumes stationary and horizontal homogeneity (Berg et al., 2022; Huettel et al., 2020), so that fluxes are assumed being conservative between the SWI and the sampling height. It integrates the flux over an extended surface of the sediment contributing to the measured fluxes, the measurement footprint (Berg et al., 2007).

The turbulent flux F of a solute is the covariance between the vertical flow velocity (w) and the solute concentration (C) measured at the same point and at the same time. Lake fluxes are typically calculated with an averaging period of about 30 min (Murniati et al., 2015), which integrates small-scale variability.

The flux computation formula is:

$$F_{AEC} = cov(w, C) = \overline{w'C'} \qquad \text{(Eq. 1)}$$

where primes indicate turbulent fluctuations computed by Reynolds decomposition ($w' = w - \overline{w}$ and $C' = C - \overline{C}$) and the overbars denote time averages.

AEC and REA (see below) instrumentation was mounted to the same frame (Fig. S1) for the common use of an acoustic Doppler velocimeter (ADV) (Vector, Nortek) and for sampling water and measuring oxygen concentration in close proximity. Velocity was measured at 8 Hz at a height of 15 cm above the sediment in order to cover the whole turbulent inertial frequency sub-range (Kaimal et al., 1972). Dissolved oxygen concentration was measured 1 cm away from the ADV sampling volume (McGinnis et al., 2008), using micro optodes (OXR430-UHS - PyroScience GmbH) sampling at 4 Hz.

AEC data post-processing began with replacing by interpolation unreliable velocity measurements with an ADV correlation between pulse and echo below 70% or a signal-to-noise ratio below 15 dB. The remaining velocity outliers were excluded and interpolated with third-order polynomials by the 3D phase space method (Goring and Nikora, 2002). In order to focus on vertical turbulent fluxes, the coordinate system of the ADV was aligned vertically by identifying the local flow plane with the planar fit method (Lorke et al., 2013; Wilczak et al., 2001). The turbulent fluctuations *w'* and *C*' were extracted

by subtracting a 60 s centred running average from the time series. This avoids interference with low-frequency non-turbulent motions, which do not contribute to the turbulent flux. Data synchronization compensates for both the distance between velocity and oxygen concentration measurement points and for the response time of the micro-optode (Lorrai et al., 2010): correlation was maximized between concentration and vertical velocity time series shifted within a 2 s window (Donis et al., 2016).

2.2. Aquatic Relaxed Eddy Accumulation

REA is based on AEC but overcomes the frequency of concentration measurements (C) and should enable a wider range of benthic fluxes to be assessed simultaneously (Lemaire et al., 2017). It replaces the fast response probes required for AEC by high frequency sampling in the TBL. REA samples conditionally, based on the fluctuation of the vertical velocity (w') compared to a threshold velocity (w_0). According to its direction, the samples are accumulated in separated reservoirs for updrafts ($w' > w_0$) and downdrafts ($w' < -w_0$) (Ammann and Meixner, 2002). The value $w_0 = 0.75\,\sigma_w$ is the best compromise for eliminating poorly characterized small eddies while sampling eddies of a large size range (Lemaire et al., 2017). The average concentrations of accumulated updrafts ($\overline{C_\uparrow}$) and downdrafts ($\overline{C_\downarrow}$) yields the flux (F):

$$F_{REA} = b\,\sigma_w\,(\overline{C_\uparrow} - \overline{C_\downarrow}) \qquad \text{(Eq. 2)}$$

where σ_w is the standard deviation of the vertical velocity, a proxy for the turbulent kinetic energy. The empirical coefficient b was shown to decrease exponentially with the ratio between w_0 and σ_w:

$$b = b_\infty + (b_0 - b_\infty) exp\left(-a\frac{w_0}{\sigma_w}\right) \text{ for } 0 \le \frac{w_0}{\sigma_w} \le 2 \qquad \text{(Eq. 3)}$$

where the empirical coefficients b_0, b_∞ and a are 0.60, 0.152 and 1.35, respectively. These values were obtained by simulating REA oxygen fluxes with AEC data (see at Lemaire et al. 2017). The technique principle was validated for oxygen fluxes (Calabro-Souza et al., 2023).

Therefore, this method requires to measure w at high frequency, while sampling water at the right time to accumulate $\overline{C_\uparrow}$ and $\overline{C_\downarrow}$ (Eq. 2 and 3). The threshold velocity w_0 used for water sampling is computed based on w'. REA works *in situ* in two separated phases: a prototype alignment period (we used 12 h, see Section S.1) and successive flux averaging periods, when the ADV imposes the water sampling frequency (at 8 Hz). At each time step, the computer discards velocities with associated correlation below 70% and calculates w' through a 30 s back-looking running average (AEC showed good agreement between fluxes obtained with 30 s back-looking and 60 s centred running averages). If $w' > w_0$, a fast response solenoid valve opens the line corresponding to the vertical velocity direction. The hydrostatic pressure difference between the inlet and outlet of the sampling line, the latter being at atmospheric pressure through a venting tube, drives samples to 300 mL plastic perfusion bags in 5 L glass bottles. At the end of each 20 min flux averaging period, w_0 was updated in order to follow the variable flow conditions, while accumulated samples were carefully recovered with a syringe through a tube installed inside each accumulation bag, immediately filtered through a 0.45 µm cellulose acetate filter and refrigerated at 6°C for transportation and storage before chemical analysis.

2.3. Mass Transfer Coefficient

Estimating benthic fluxes from the waterside concentration gradient requires knowledge about the DBL thickness, which becomes difficult to measure in situ (Lorke et al., 2003). To overcome this, it is common practice in environmental engineering to simplify Fick's first law of diffusion by the application of a mass transfer coefficient, also called transfer velocity. It combines the effects of turbulence (on the thickness of the diffusive boundary layer) and the solute-specific diffusion coefficient into a single parameter (Boudreau and Jorgensen, 2001; Thibodeaux et al., 2011):

$$F_{MTC} = -K(C_{TBL} - C_{SWI}) \qquad \text{(Eq. 4)}$$

where K is the mass transfer coefficient (m s^{-1}) and C_{TBL} and C_{SWI} are the solute concentrations (mmol L^{-1}) measured within the TBL and at the SWI, respectively. Theoretical arguments and empirical evidence suggest that the mass transfer coefficient can be expressed as:

$$K = \alpha\, u_* Sc^{\beta} \qquad \text{(Eq. 5)}$$

, where α and β are empirical coefficients, u_* is the friction velocity (m s^{-1}), and Sc is the dimensionless Schmidt number expressing the ratio between water kinematic viscosity (m^2 s^{-1}) and solute molecular diffusivity D (m^2 s^{-1}) (Shaw and Hanratty, 1977; Lorke and Peeters, 2006). While α represents the (momentum) transfer resistance, β is linked to the rigidity and roughness of the interface (Jähne et al., 1987). Based on flume experiments with synthetic sediments, O'Connor and Hondzo (2008) recommended $\alpha = 0.164$ and $\beta = -2/3$, which were validated later by surface renewal theory (O'Connor et al., 2009).

The friction velocity considering both longitudinal and lateral velocity directions is defined as in Weber (1999):

$$u_* = \sqrt[4]{\overline{u'w'}^2 + \overline{v'w'}^2} \qquad \text{(Eq. 6)}$$

the primes denote the fluctuation of the velocity components u, v and w corresponding to the longitudinal, lateral and vertical directions, respectively.

Therefore, implementing the MTC method requires estimates of the average concentrations at the SWI (C_{SWI}) and in the TBL (C_{TBL}), friction velocity (u_*), and water temperature (Eq. 4 and 5). The latter affects solute diffusivity and water viscosity. Ion molecular diffusivity was computed based on its relation to molecular weight and absolute ion valence as described in Thibodeaux et al. (2011).

C_{SWI} was measured with a diffusive equilibrium thin-layer (DET) (Krom et al., 1994) adapted to be set horizontally on the sediment surface, from now on called "interface peepers". Two 5 x 20 x 4 mm pieces of BPA-I gel (Zhang and Davison, 1999) were sandwiched between two 0.4 µm thick dialysis membranes inside a plastic, 3D printed frame. Besides preventing the intrusion of particles into the gel, this setup allows vertical diffusion through both sides of the gel, contrary to the usual DETs. The frame was placed horizontally at the lake bottom with the help of fishing line and weights, while assisted by an underwater camera (Fig. S2). Whereas the interface peeper disturbs the DBL locally, pilot tests in lab-incubated sediments with water stirring showed agreement between C_{SWI} measured by vertical and horizontal minipeepers (unpublished results). *In-situ* deployment considered five interface peepers randomly distributed on the sediment surface around the REA and AEC instruments (around 5 m apart) for 6 to 8 h exposure time before retrieval with the fishing line.

C_{TBL} was estimated from 6 x 2.5 L samples taken from the water accumulated for REA. These were immediately filtered, with a 0.22 µm polyether-sulfone filter, and preserved at 6 °C before their chemical analysis as described below.

Friction velocities u_* were estimated, as close as possible to the SWI (around 7 cm), from measurements collected at 16 Hz from a second ADV (Vector, Nortek) set in a side-looking position on an independent frame to avoid bottom reflection (Fig. S3). Velocities were processed as for AEC, with a running average window of 5 min.

2.4. Fick's law in incubated sediment cores

This method assumes that molecular diffusion prevails over turbulent diffusion right at the SWI. Such assumption is valid for fine sediments under low flow conditions (Grant et al., 2020). Then, if the interfacial gradient of solute concentrations is known, benthic fluxes can be estimated by applying Fick's first law of diffusion:

$$F = -D\frac{\partial C}{\partial z}, \qquad \text{(Eq. 7)}$$

where D is the solute molecular diffusivity, C is the solute concentration in the diffusive sublayer (Lorke and MacIntyre, 2009), and z is the vertical coordinate. Both porosity and tortuosity effects are absent right at the sediment surface.

Benthic fluxes were also assessed by incubating three sediment cores (8.5 cm in diameter, 25 cm of sediment and 25 cm of lake water) collected near the MTC, REA and AEC sampling area (about 10 m apart). These were incubated in the lab (Fig. S7) under constant 20°C, open to air at the top (lake bottom temperature was 22.1 °C, showing oxygen super-saturation) and exposed to indirect, natural light for five days before measurements. To reproduce lake mixing during measurements, core water was recirculated for two hours before measurements with an additional volume that had been collected from the lake in equal proportions under the surface, at mid-depth and at the bottom of the water column. This prevented the accumulation of solutes in the free water phase; the recirculating volume was equivalent to the volume of water column over the cored sediment in the lake (56 L). The three cores were connected to the same recirculating water system (in parallel) using polyethylene tubes (4 mm diameter) and an aquarium pump (0.17 L min^{-1}). The inflow tube poured water on top of each core, while the outflow tube was placed 15 cm below water surface. The main velocity of recirculation in each core was estimated to be ~ 1 mm s^{-1}. Water recirculation was confirmed visually by rhodamine dye tracing.

DETs of 100 x 25 x 4 mm BPA-I gel were exposed for 12 h in the cores. Once recovered and rinsed, the gel was sliced into 5 mm layers. Each slice was placed in a pre-weighted glass vial and diluted with 2.5 mL mili-Q water, then stored horizontally for 18 h to keep the gel saturated. Then the slices were transferred to other vials with a 2.5 mL 1% nitric acid solution and let back diffuse into the solution for another 18 h before being discarded. Both water and acid solutions were analysed to determine the concentration of dissolved compounds. During DET exposition, an oxygen microprofile was measured with a micro-optode (PSt7, PreSens, Germany) operated with a micromanipulator (accuracy 10 µm) with 100 µm and 60 s steps for equilibration.

Benthic fluxes from sediment incubations were estimated using Eqn. 7, where the interfacial gradients were obtained by linear regressions of the concentration profiles. For the oxygen microprofile, only points located within the DBL were used. Since minipeepers fail to monitor the DBL, the number of regression points for other solutes was chosen to maximize the coefficient of determination.

2.5. Chemical analysis

The target benthic fluxes of this comparison were ammonium, phosphate, iron and manganese, as the two key nutrients regulating primary production and the two key metallic, alternative terminal electron-acceptors for anaerobic respiration. Nitrate, nitrite, total dissolved phosphorus and sulphate were also analysed for a complete picture of chemical gradients in porewater. Anion concentrations of REA samples were analysed by ion chromatography (Compact flex 930, Metrohm AG, accuracy of 1% for concentration differences analysis), while ammonium by UV-visible spectrophotometry (Lambda 35, Perkin Elmer Inc., accuracy 5%). PO_4^{3-}, NO_3^-, NO_2^-, SO_4^{2-} and NH_4^+ concentrations for MTC and sediment porewater samples were analysed by ion chromatography (ICS 3000 Dionex, Thermo Fisher Scientific Inc., accuracy 5%). For iron and manganese ions, all samples were analysed by inductively coupled plasma mass spectrometry (ICP-MS, Agilent 8800 ICP-QQQ, accuracy 15%). Samples obtained after acid dilution were analysed only by ICP-MS.

2.6. Assessment and other methodological aspects

In order to assess the performance of REA and MTC techniques *in situ* (Figure 1), we compared their fluxes to each other in a hypereutrophic shallow urban lake (mean depth: 2.5 m). As a reference, we also compared them with values from sediment incubation and AEC (oxygen fluxes).

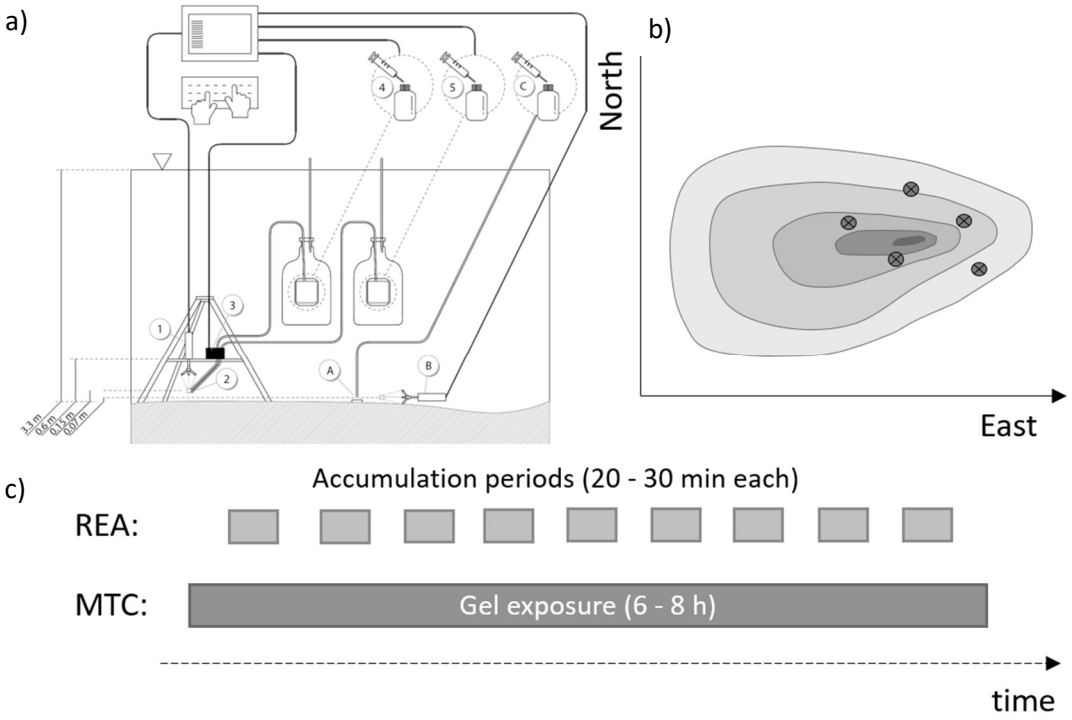

Figure 1 - Relaxed Eddy Accumulation (REA) and Mass Transfer Coefficient (MTC) techniques work at different spatiotemporal scales: a) REA measures fluctuating vertical velocities with acoustic Doppler velocimetry (ADV) to accumulate upwards ($\overline{C_\uparrow}$) and downwards ($\overline{C_\downarrow}$) concentrations that are collected close to the sediment (15 cm) surface but within the turbulent boundary layer (TBL). MTC also relies on a TBL solute concentration, C_{TBL}, and the concentration at the sediment-water interface (SWI), C_{SWI}. It measures friction velocity as close to bottom as possible with a side-looking ADV, at 7 cm in this case. Numbers in panel a) represent REA components: (1) ADV, (2) sampling needles, (3) solenoid valves, (4) updraft sample, and (5) downdraft sample. Letters represent MTC components: (A) interface peeper, (B) ADV, and (C) water sample. b) REA point measurements yield benthic fluxes that represent a sediment footprint (contour lines schematically representing areas contributing equally to fluxes) of about 200 m² in this case, whereas MTC scattered point measurements are only representative for those locations (dark crossed circles) - assuming that they are exposed to similar hydrodynamics. (c) While REA provides benthic fluxes that represent flux averaging periods of 20 to 30 min duration, MTC fluxes are representative for the gel exposure time of 6 – 8 h.

Additional methodological aspects can be found in Supplementary Material. These include: i) flux quality analysis for REA and AEC, ii) estimation of flux uncertainty, iii) considerations on spatiotemporal scales, and iv) study site.

3. Results

3.1. Hydrodynamic conditions

The lake was stratified during measurements. Hydrodynamic conditions characterized by friction velocity (Figure 2) showed relatively low turbulence with values fluctuating up to 0.4 cm s-1. Measurements at 7 cm above the sediment (used for MTC) and at 15 cm (used for REA) exhibited comparable magnitudes, at least for the first four hours.

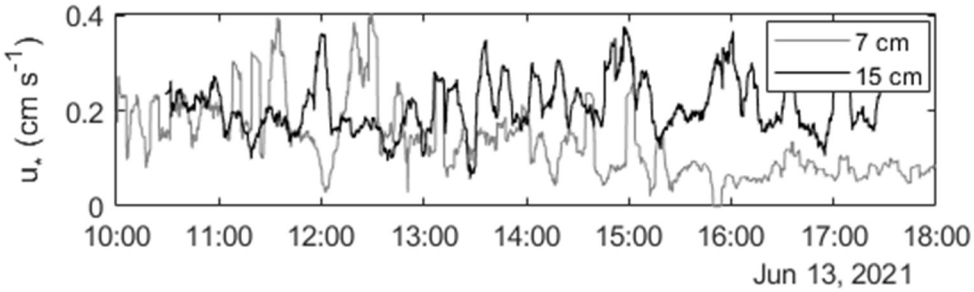

Figure 2 - Hydrodynamic conditions described by friction velocity (u) during the measurements of benthic fluxes. Time series were smoothened by a 5-min moving average. Data collected by acoustic Doppler velocimetry at 7 and 15 cm above the sediment bed used for Relaxed Eddy Accumulation and Mass Transfer Coefficient methods, respectively*

3.2. REA measurements suggest sub-daily flux dynamics

Figure 3h indicates which part of the velocity distribution was sampled by REA during each flux-averaging period, conforming the symmetrical sampling of updrafts and downdrafts. Results show an hourly dynamic of the benthic fluxes of nutrients and metallic ions (Figure 3 b-e). Ammonium, manganese, and iron show a similar oscillating pattern of negative, positive and again negative fluxes. The trend is more questionable for phosphate fluxes due to large uncertainties. These ion fluxes follow a different dynamic in time than oxygen fluxes (Figure 3a, consistently always negative) and turbulence indicated by friction velocities (Figure 2). Significant correlations were observed between phosphate and ammonium fluxes, (Figure 3f - $R^2 = 0.73$), as well as between iron and manganese fluxes, (Figure 3g - $R^2 = 0.72$).

The prototype alignment duration (12 h) was sufficient for aligning the REA prototype to the vertical (see Section S.1 in Supp. Info.), and practical since the equipment can be deployed the day before sampling.

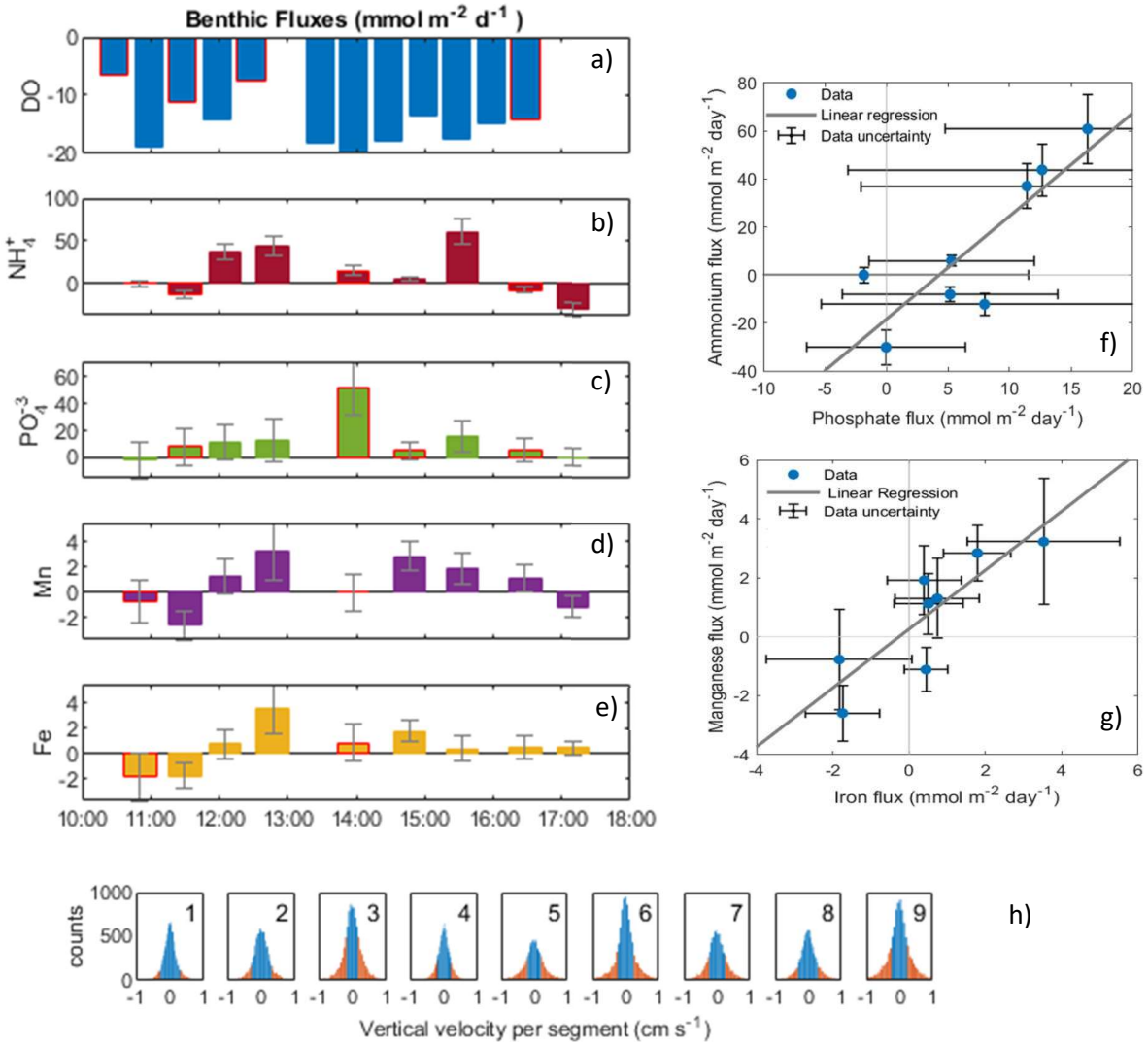

Figure 3 - Benthic fluxes measured with Relaxed Eddy Accumulation (REA) suggest daily dynamics in nutrient and metallic ions. Panels a) to e): flux sign refers to its direction, being positive towards the water column; error bars represent flux uncertainty; fluxes computed with low confidence marked by red contours. Intercomparison of REA fluxes shown in panels f) Ammonium and Phosphate (R2 = 0.73, y = 4.286x - 18.36) and g) Manganese and Iron (R2 = 0.72 - y = 0.9997x + 0.2625). Panel h): histograms of vertical velocities during each flux-averaging period (1 to 9) show in red those values exceeding the vertical velocity thresholds for REA sampling.

3.3. MTC interface peepers reveals sediment heterogeneity

Table 1 presents the parameters used for estimating benthic fluxes by the MTC method. Capturing the actual *in-situ* interfacial concentration is crucial for estimating benthic fluxes by the MTC method, as we expect it to be the most uncertain parameter. Compared to sediment incubation results (Fig. S5Figure), interface peepers seem to capture *in-situ* interfacial concentrations (except for sulphate): differing by 76, 62, 6, and 22%, respectively, for ammonium, phosphate, manganese, and iron ions. This parameter (C_{SWI}) showed a larger variability in space (gels were exposed about 5 m apart) than concentrations in the water column (C_{TBL}) during the day (average coefficients of variation of 104 and 28%, respectively). This shows a potential degree of heterogeneity of the sediment surface.

Table 1 - Parameters involved in the calculation of benthic fluxes by the mass transfer coefficient (MTC) method, as well as its resulting fluxes. C_{TBL} and C_{SWI} are concentrations in the turbulent boundary layer and at the sediment-water interface, respectively. Mean values and standard deviations were computed out of seven water samples and five interface peepers, respectively, for C_{TBL} and C_{SWI}. The Schmidt number was computed considering each solute's diffusion coefficient (Table S2) plus temperature-corrected water viscosity (9.638 x 10^{-7} m^2 s^{-1} at 22.2°C).

Compound	Friction velocity (cm s^{-1})	Schmidt number (-)	K (10^{-6} m s^{-1})	C_{TBL} (mmol m^{-3})	C_{SWI} (mmol m^{-3})	Flux (mmol m^{-2} d^{-1})
Ammonium	0.15 ± 0.08	558	3.6 ± 1.9	0.6 ± 0.3	135.4 ± 44	42.24 ± 25.69
Phosphate		1221	2.2 ± 1.1	1.8 ± 0.3	2.9 ± 1.4	0.22 ± 0.29
Iron		924	2.6 ± 1.3	0.04 ± 0	3.3 ± 4.1	0.76 ± 1.51
Manganese		922	2.6 ± 1.3	0.02 ± 0	3.4 ± 6.5	0.73 ± 0.99

3.4. Sediment incubation show the difficulty to reproduce natural conditions

As expected, porewater concentrations of nutrients and metallic ions show strong gradients at the sediment-water interface, with changes of one order of magnitude within a few centimetres (Fig. S5). This facilitates the estimation of benthic fluxes by Fick's law, as summarised in Table S2. Besides flux quantification, these concentration profiles give us an insight of the biogeochemical processes occurring at the SWI, supporting the interpretation of MTC and REA fluxes. For instance, we observe that oxygen is consumed in the upper millimetre of the sediment surface (Fig. S5a) but significant organic matter decomposition rates should still occur down to 3 cm. This is reflected by the stabilization of porewater concentrations of those elements that are released or consumed during OM decomposition (see P, PO_4^{3-}, NH_4^+, Mn, and SO_4^{2-}) below this depth. Microbial activity also leads to accumulation of solutes at certain layers. Nitrate accumulates at about 1 cm below the interface due strong uptake in the upper oxic layers plus denitrification in the lower anoxic layers. Meanwhile, nitrite accumulates about 0.5 cm above the interface due constant ammonia oxidation under aerobic conditions, because nitrite is an intermediate oxidation state before the complete oxidation of ammonia into nitrate.

3.5. Consistency among methods

Average benthic fluxes measured with REA (time averages) are of the same order of magnitude than MTC fluxes for ammonium (23.5 and 42.2 mmol m^2 d^{-1}), manganese (1.0 and 0.8 mmol m^2 d^{-1}), and iron (0.8 and 0.7 mmol m^2 d^{-1}) (Figure 4 and Table S3). The large discrepancy of phosphate fluxes, of more than an order of magnitude (7.7 and 0.2 mmol m^{-2} d^{-1}), could be attributed to overestimated REA concentration differences due to analytical accuracy.

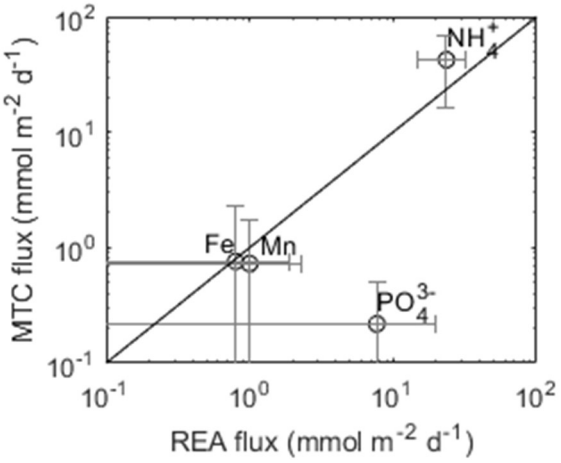

Figure 4 - Comparison of non-invasive methods for estimating benthic fluxes of different solutes: Relaxed Eddy Accumulation (REA) and Mass Transfer Coefficient (MTC). The diagonal line represents the ideal case with equal fluxes. Circle points show mean values and error bars represent flux uncertainty. Measurements were performed at Lake Champs on 13 June 2021 under *in-situ* hydrodynamic conditions.

Nutrient fluxes obtained by REA and MTC (23.5 to 42.2 for ammonium and 0.2 to 7.7 mmol m^{-2} d^{-1} for phosphate) are in the range of literature values from similar waterbodies, estimated by different methods (1.6 to 72 for ammonium and 0.2 to 8.4 mmol m^{-2} d^{-1} for phosphate, see Table S4). In the case of ammonium, REA and MTC fluxes fall within the upper literature range.

Roughly, ion fluxes from sediment incubations are by one or two orders of magnitude lower than MTC and average REA fluxes (Table S3). Meanwhile, the downward oxygen flux of 36.4 mmol m^2 d^{-1} measured during sediment incubation (Fig. S5, Table S3) is more than the double of the average AEC flux (14.6 mmol m^2 d^{-1}, Figure 3a, Table S3) measured *in situ*.

4. Discussion

4.1. Can we reliably measure benthic fluxes in situ?

Naturally, the answer to this question depends on the accuracy required when assessing a given scientific hypothesis. In this study, we obtained comparable benthic fluxes of ammonium, iron and manganese ions measured by REA and MTC methods (Figure 4). This level of accuracy is acceptable for a first attempt that should improve with continued practice. Nutrient fluxes are consistent with values found in literature, with ammonium fluxes falling in the upper range (see Table S4). Flux values for sediment incubations were by one or two orders of magnitude lower than for REA and MTC (Table S3). This difference may be attributed to our inability to replicate both lake turbulence and oxygen levels in the lab. Oxygen was depleted at 15 cm above the sediment in the lake (17% saturation rate) but close to saturation in the lab incubation (92%). Another reason for this underestimation of fluxes at lab could be the vertical resolution of the minipeepers used to resolve the interfacial gradients (5 mm): concentration gradients could have been steeper than measured, and fluxes larger.

The TBL solute concentrations used for REA (Table S1) were higher than for MTC (Table 1) by 66, 115, 19, and 79% for NH_4^+, PO_4^{3-}, Fe, and Mn ions, respectively. We attribute these differences to two main factors: samples were filtered through different pore sizes (0.45 µm for REA vs 0.22 µm for MTC) and were analysed in different laboratories. Such discrepancies lead to biases in the presented comparison between REA and MTC fluxes. However, since the estimation of fluxes by REA depends

on concentration differences - rather than on absolute values - we considered it worth to perform this comparison.

REA system requires a minimum level of turbulence to work properly. Previous work suggests a minimum working threshold for friction velocities above 0.5 x 10^{-3} m s^{-1} (Calabro-Souza et al., 2023). In this study, the power spectra of the vertical velocity showed a clear turbulent inertial subrange for all flux-averaging periods.

In general, we expect that eutrophic conditions favour high benthic fluxes, measurable by REA and MTC, due to an active sediment microbial community dwelling under high settling rates of organic matter. On the contrary, in oligotrophic waters benthic fluxes may be too small to be captured, because concentrations differences ($\overline{C_{\uparrow}} - \overline{C_{\downarrow}}$ and $C_{SWI} - C_{TBL}$) may fall below detection level. As a reference, Maassen et al. (2005) reported interfacial concentration gradients of soluble reactive P to be one order of magnitude higher in eutrophic systems than in oligotrophic systems. If so, these techniques would be more suitable for monitoring benthic fluxes in eutrophic rather than in oligotrophic systems. Furthermore, the potential for measuring fluxes of other - detectable – compounds or pollutants is yet to be assessed.

4.2. Challenges

REA consistently captured benthic fluxes, except for phosphate for which difficulties in detecting small concentration differences cause large uncertainties. Phosphate analytical accuracy (1%) exceeded the measured relative concentration differences during half of the flux-averaging periods (Table S1) (it was also the case for sulphate, data not shown). Dilution and pre-concentration of samples before chemical analysis could be used in order to magnify these concentration differences (Okumura et al., 1998; Telliard, 1997).

REA relies on velocity alignment. In this shallow lake, planar fit required a 12 h alignment due to low turbulence. While this duration may seem long compared to a REA application in a stream, which typically takes few minutes, the system can be deployed one day ahead of flux measurements.

The MTC method - as applied here - presents similar limitations as for DETs (Zhang and Davison, 1999), because it uses a similar gel. This affects the flux estimation in terms of its spatiotemporal resolution. Whereas the spatial representation can be enlarged by increasing the number of samplers deployed, the covered area should preserve certain hydrodynamic homogeneity. In our case, interfacial concentrations agreed between laboratory and field estimations, except for sulphate (Fig. S5). Regarding the time scale, MTC averages fluxes that can change significantly during gel exposition, just as REA results suggest (Figure 3). Flux changes may be attributed to changes in sediment biogeochemistry coupled with hydrodynamics. Therefore, we recommend exposing gels under quasi-steady conditions of both aspects, e.g. stable sedimentation rates and wind conditions.

The quality of friction velocity measurements required for MTC is questionable when velocity fluctuations are small and approach the noise level of the instrument (± 0.5% of measured value ± 1 mm s^{-1}), as it is common in standing waters. We recommend examining the power spectral density functions of the three velocity components in both logarithmic and variance-preserving forms. In particular, (i) to check that a -5/3 slope appears in logarithmic scales, revealing the existence of an inertial subrange, and (ii) to assure on variance-preserving power spectra that the ADV captures all turbulent energy within the measured frequency domain. Noisy data would show a distortion of these expected patterns (Durgesh et al., 2014) (Fig. S6).

Moreover, the K vs u_* relation (Eq. 5) used by the MTC method lacks experimental validation for low-flow velocities, close to laminar flow. Lorke and Peeters (2006) assessed this scaling relationship for values above 0.25 cm s^{-1}, while we applied it for 0.15 cm s^{-1}. Their assessment showed uncertainties of one order of magnitude in the transfer velocity for low friction velocities, which would result in a comparable uncertainty as in our flux estimates. However, we used the parameters suggested by O'Connor and Hondzo (2008) and the smallest friction velocity considered in their experiments was the same as ours, 0.15 cm s^{-1}. This point deserves further investigation.

The potential of both the REA and MTC techniques for measuring fluxes of other compounds is yet to be assessed.

4.3. Capabilities

Besides REA and MTC limitations, both methods offer complementary capabilities for characterizing the dynamics of benthic fluxes and its main drivers. For instance, REA could contribute to explore the temporal variation at a relatively short time-scale (< 1 h), covering a large sediment surface (~ 100 m^2) that integrates any small-scale variability. Meanwhile, several minipeepers, exposed simultaneously for MTC within the REA footprint area, should resolve the spatial variability of fluxes.

5. Conclusions

This study assessed the performance of two promising non-invasive techniques for measuring benthic fluxes *in situ*: relaxed eddy accumulation (REA) and mass transfer coefficient (MTC). For the first time, REA revealed hourly flux variations, indicating a strong lake biogeochemical dynamic at short time-scales. Daily-averaged fluxes measured by MTC and REA were comparable in magnitude for ammonium (24 and 42 mmol m^2 d^{-1}), manganese (1.0 and 0.8 mmol m^2 d^{-1}) and iron (0.8 and 0.7 mmol m^2 d^{-1}), while phosphate fluxes differed by one order of magnitude (7.7 and 0.2 mmol m^2 d^{-1}), probably due to higher analytical uncertainties. These fluxes fall within the range of fluxes reported for similar water bodies and estimated by other methods. The use of several interface peepers for the MTC method addresses the potentially high spatial sediment and flux heterogeneity of benthic fluxes at the meter-scale. Although the accuracy of both techniques needs to be improved, the results show their potential for a better empirical characterization of the effects of hydrodynamic conditions on benthic fluxes. They can support both scientific and applied research in several fields of limnology and water pollution. For instance, REA could help describe the short-term biogeochemical dynamics of sediments thanks to its sub-hourly sampling capabilities. Meanwhile, MTC could be used for lake monitoring and management because of its relatively simple implementation.

Acknowledgements

Guilherme Calabro Souza and Felipe Breton received a doctoral scholarship from École des Ponts ParisTech and Jihočeská Univerzita, respectively. The subaquatic REA development project received financial support from AgroParisTech and OSU EFLUVE. The Czech Ministry of Agriculture partly financed this work by the project QK22020179 and the Ministry of Environment by project SS06020167.

The authors thank: Base de Loisirs de Champs-sur-Marne for technical assistance; interns Celia Ramos Sanchez and Clément Molinier for their contribution to preliminary measurements; Paul-Adrian Bulzu for advice with benthic-water sampling; Vivien Roussel for support with 3D-printing; Antoine Lefur for graphic design of diagrams; Lila Boudahmane, Tomáš Hubáček, Olivier Lauret, and Mohamed Saad for the chemical analysis of water samples; Christophe Rabouille's team for facilitating their coring device; and Nana Osafo, Didier Jézéquel and Eric Viollier for fruitful discussions.

References

Ammann, C., Meixner, F., 2002. Stability dependence of the relaxed eddy accumulation coefficient for various scalar quantities. Journal of Geophysical Research: Atmospheres 107, ACL7-1.

Berg, P., Huettel, M., Glud, R.N., Reimers, C.E., Attard, K.M., 2022. Aquatic eddy covariance: the method and its contributions to defining oxygen and carbon fluxes in marine environments. Annual Review of Marine Science 14.

Berg, P., Long, M.H., Huettel, M., Rheuban, J.E., McGlathery, K.J., Howarth, R.W., Foreman, K.H., Giblin, A.E., Marino, R., 2013. Eddy correlation measurements of oxygen fluxes in permeable sediments exposed to varying current flow and light. Limnology and Oceanography 58, 1329–1343. https://doi.org/10.4319/lo.2013.58.4.1329

Berg, P., Pace, M.L., 2017. Continuous measurement of air–water gas exchange by underwater eddy covariance. Biogeosciences 14, 5595–5606. https://doi.org/10.5194/bg-14-5595-2017

Berg, P., Risgaard-Petersen, N., Rysgaard, S., 1998. Interpretation of measured concentration profiles in sediment pore water. Limnology and Oceanography 43, 1500–1510.

Berg, P., Røy, H., Janssen, F., Meyer, V., Jørgensen, B.B., Huettel, M., de Beer, D., 2003. Oxygen uptake by aquatic sediments measured with a novel non-invasive eddy-correlation technique. Marine Ecology Progress Series 261, 75–83.

Berg, P., Røy, H., Wiberg, P.L., 2007. Eddy correlation flux measurements: The sediment surface area that contributes to the flux. Limnology and Oceanography 52, 1672–1684.

Boudreau, B.P., Guinasso, N.L., 1981. The influence of a diffusive sublayer on accretion, dissolution, and Diagenesis at the sea floor, in The Dynamic Environment of the Ocean Floor (Fanning, KA, and Manheim, FT, eds.).

Boudreau, B.P., Jorgensen, B.B., 2001. The benthic boundary layer: Transport processes and biogeochemistry.

Boynton, W.R., Ceballos, M.A.C., Bailey, E.M., Hodgkins, C.L.S., Humphrey, J.L., Testa, J.M., 2017. Oxygen and Nutrient Exchanges at the Sediment-Water Interface: a Global Synthesis and Critique of Estuarine and Coastal Data. Estuaries and Coasts 41, 301–333. https://doi.org/10.1007/s12237-017-0275-5

Bryant, L.D., Lorrai, C., McGinnis, D.F., Brand, A., est, A.W., Little, J.C., 2010. Variable sediment oxygen uptake in response to dynamic forcing. Limnology and Oceanography 55, 950–964.

Calabro-Souza, G., Lorke, A., Noss, C., Dubois, P., Saad, M., Ramos-Sanchez, C., Vinçon-Leite, B., Moilleron, R., Jodeau, M., Lemaire, B.J., 2023. A New Technique for Resolving Benthic Solute Fluxes: Evaluation of Conditional Sampling Using Aquatic Relaxed Eddy Accumulation. Earth and Space Science 10, e2023EA003041. https://doi.org/10.1029/2023EA003041

Cheng, X., Zeng, Y., Guo, Z., Zhu, L., 2014. Diffusion of nitrogen and phosphorus across the sediment-water interface and in seawater at aquaculture areas of Daya Bay, China. International journal of environmental research and public health 11, 1557–1572.

Coogan, J., Rheuban, J.E., Long, M.H., 2022. Evaluating benthic flux measurements from a gradient flux system. Limnology and Oceanography: Methods 20, 222–232. https://doi.org/10.1002/lom3.10482

Dade, W.B., 1993. Near-bed turbulence and hydrodynamic control of diffusional mass transfer at the sea floor. Limnology and Oceanography 38, 52–69.

de Beer, D., 2011. Microsensors for Sediments, Microbial Mats, and Biofilms, in: Encyclopedia of Geobiology. Springer, pp. 658–662.

Di Toro, D.M., 2001. Sediment flux modeling. Wiley-Interscience New York.

Ding, Y., Qin, B., Deng, J., Ma, J., 2017. Effects of episodic sediment resuspension on phytoplankton in Lake Taihu: Focusing on photosynthesis, biomass and community composition. Aquatic Sciences 79, 617–629.

Donis, D., McGinnis, D.F., Holtappels, M., Felden, J., Wenzhoefer, F., 2016. Assessing benthic oxygen fluxes in oligotrophic deep sea sediments (HAUSGARTEN observatory). Deep Sea Research Part I: Oceanographic Research Papers 111, 1–10. https://doi.org/10.1016/j.dsr.2015.11.007

Durgesh, V., Thomson, J., Richmond, M.C., Polagye, B.L., 2014. Noise correction of turbulent spectra obtained from acoustic doppler velocimeters. Flow Measurement and Instrumentation 37, 29–41. https://doi.org/10.1016/j.flowmeasinst.2014.03.001

Emerson, S., Hedges, J., 2003. Sediment Diagenesis and Benthic Flux, in: Holland, H.D., Turekian, K.K. (Eds.), Treatise on Geochemistry. Pergamon, Oxford, pp. 293–319. https://doi.org/10.1016/B0-08-043751-6/06112-0

Fan, J., Wang, D., Zhang, K., 2010. Experimental study on a dynamic contaminant release into overlying water-body across sediment-water interface. Journal of Hydrodynamics 22, 343–346. https://doi.org/10.1016/s1001-6058(09)60218-3

Glud, R.N., Berg, P., Thamdrup, B., Larsen, M., Stewart, H.A., Jamieson, A.J., Glud, A., Oguri, K., Sanei, H., Rowden, A.A., Wenzhöfer, F., 2021. Hadal trenches are dynamic hotspots for early diagenesis in the deep sea. Commun Earth Environ 2, 1–8. https://doi.org/10.1038/s43247-020-00087-2

Goring, D.G., Nikora, V.I., 2002. Despiking acoustic Doppler velocimeter data. Journal of Hydraulic Engineering 128, 117–126.

Grant, S.B., Azizian, M., Cook, P., Boano, F., Rippy, M.A., 2018. Factoring stream turbulence into global assessments of nitrogen pollution. Science 359, 1266–1269.

Grant, S.B., Gomez-Velez, J.D., Ghisalberti, M., Guymer, I., Boano, F., Roche, K., Harvey, J., 2020. A One-Dimensional Model for Turbulent Mixing in the Benthic Biolayer of Stream and Coastal Sediments. Water resources research 56. https://doi.org/10.1029/2019wr026822

Gu, X., Chen, K., Zhang, L., Fan, C., 2016. Preliminary evidence of nutrients release from sediment in response to oxygen across benthic oxidation layer by a long-term field trial. Environmental Pollution 219, 656–662. https://doi.org/10.1016/j.envpol.2016.06.044

Hesslein, R.H., 1976. An in situ sampler for close interval pore water studies 1. Limnology and oceanography 21, 912–914.

Huettel, M., Berg, P., Merikhi, A., 2020. Measurements and data analysis of sediment–water oxygen flux using a new dual-optode eddy covariance instrument. Biogeosciences 17, 4459–4476.

Imboden, D.M., Wüest, A., 1995. Mixing mechanisms in lakes, in: Physics and Chemistry of Lakes. Springer, pp. 83–138.

Jähne, B., Münnich, K.O., Bösinger, R., Dutzi, A., Huber, W., Libner, P., 1987. On the parameters influencing air-water gas exchange. Journal of Geophysical Research: Oceans 92, 1937–1949.

Jiang, Q., Jin, G., Tang, H., Xu, J., Jiang, M., 2022a. Ammonium (NH4+) transport processes in the riverbank under varying hydrologic conditions. Science of The Total Environment 826, 154097. https://doi.org/10.1016/j.scitotenv.2022.154097

Jiang, Q., Kaufman, M.H., Jin, G., Tang, H., Xu, J., 2022b. Transition Zone Morphology Dynamics of Dissolved Oxygen (DO) in a Salinity-Impacted Hyporheic Zone. Geophysical Research Letters 49, e2022GL099932. https://doi.org/10.1029/2022GL099932

Jin, G., Chen, H., Zhang, Z., Jiang, Q., Liu, Z., Tang, H., 2022. Transport of Phosphorus in the Hyporheic Zone. Water Resources Research 58, e2021WR031292. https://doi.org/10.1029/2021WR031292

Kaimal, J.C., Wyngaard, J., Izumi, Y., Coté, O., 1972. Spectral characteristics of surface-layer turbulence. Quarterly Journal of the Royal Meteorological Society 98, 563–589.

Koelmans, A.A., Poot, A., Lange, H.J.D., Velzeboer, I., Harmsen, J., Noort, P.C.M. van, 2010. Estimation of In Situ Sediment-to-Water Fluxes of Polycyclic Aromatic Hydrocarbons, Polychlorobiphenyls and Polybrominated Diphenylethers [WWW Document]. ACS Publications. https://doi.org/10.1021/es903938z

Kononets, M., Tengberg, A., Nilsson, M., Ekeroth, N., Hylén, A., Robertson, E.K., van de Velde, S., Bonaglia, S., Rütting, T., Blomqvist, S., Hall, P.O.J., 2021. In situ incubations with the Gothenburg benthic chamber landers: Applications and quality control. Journal of Marine Systems 214, 103475. https://doi.org/10.1016/j.jmarsys.2020.103475

Krom, M.D., Davison, P., Zhang, H., Davison, W., 1994. High-resolution pore-water sampling with a gel sampler. Limnology and Oceanography 39, 1967–1972.

Lemaire, B.J., Noss, C., Lorke, A., 2017. Toward relaxed eddy accumulation measurements of sediment-water exchange in aquatic ecosystems. Geophysical Research Letters 44, 8901–8909. https://doi.org/10.1002/2017gl074625

Lerman, A., 1978. Chemical exchange across sediment-water interface. Annual Review of Earth and Planetary Sciences 6, 281.

Long, M.H., Charette, M.A., Martin, W.R., McCorkle, D.C., 2015. Oxygen metabolism and pH in coastal ecosystems: Eddy Covariance Hydrogen ion and Oxygen Exchange System (ECHOES). Limnology and Oceanography: Methods 13, 438–450. https://doi.org/10.1002/lom3.10038

Lorke, A., MacIntyre, S., 2009. The benthic boundary layer (in Rivers, Lakes, and Reservoirs), in: Encyclopedia of Inland Waters. Oxford: Elsevier, pp. 505–514.

Lorke, A., McGinnis, D.F., Maeck, A., 2013. Eddy-correlation measurements of benthic fluxes under complex flow conditions: Effects of coordinate transformations and averaging time scales. Limnology and Oceanography: Methods 11, 425–437. https://doi.org/10.4319/lom.2013.11.425

Lorke, A., Müller, B., Maerki, M., Wüest, A., 2003. Breathing sediments: The control of diffusive transport across the sediment-water interface by periodic boundary-layer turbulence. Limnology and Oceanography 48, 2077–2085.

Lorke, A., Peeters, F., 2006. Toward a unified scaling relation for interfacial fluxes. Journal of physical oceanography 36, 955–961.

Lorrai, C., McGinnis, D.F., Berg, P., Brand, A., Wüest, A., 2010. Application of oxygen eddy correlation in aquatic systems. Journal of Atmospheric and Oceanic Technology 27, 1533–1546.

Maassen, S., Uhlmann, D., Röske, I., 2005. Sediment and pore water composition as a basis for the trophic evaluation of standing waters. Hydrobiologia 543, 55–70. https://doi.org/10.1007/s10750-004-5946-0

Mackay, E.B., Folkard, A.M., Jones, I.D., 2014. Interannual variations in atmospheric forcing determine trajectories of hypolimnetic soluble reactive phosphorus supply in a eutrophic lake. Freshwater biology 59, 1646–1658.

McGinnis, D.F., Berg, P., Brand, A., Lorrai, C., Edmonds, T.J., Wüest, A., 2008. Measurements of eddy correlation oxygen fluxes in shallow freshwaters: Towards routine applications and analysis. Geophysical Research Letters 35. https://doi.org/10.1029/2007gl032747

McGinnis, D.F., Cherednichenko, S., Sommer, S., Berg, P., Rovelli, L., Schwarz, R., Glud, R.N., Linke, P., 2011. Simple, robust eddy correlation amplifier for aquatic dissolved oxygen and hydrogen sulfide flux measurements. Limnology and Oceanography: Methods 9, 340–347. https://doi.org/10.4319/lom.2011.9.340

Murniati, E., Geissler, S., Lorke, A., 2015. Short-term and seasonal variability of oxygen fluxes at the sediment–water interface in a riverine lake. Aquatic Sciences 77, 183–196.

Mustajärvi, L., Eek, E., Cornelissen, G., Eriksson-Wiklund, A.-K., Undeman, E., Sobek, A., 2017. In situ benthic flow-through chambers to determine sediment-to-water fluxes of legacy hydrophobic organic contaminants. Environmental Pollution 231, 854–862. https://doi.org/10.1016/j.envpol.2017.08.086

O'Connor, B.L., Hondzo, M., 2008. Dissolved oxygen transfer to sediments by sweep and eject motions in aquatic environments. Limnology and Oceanography 53, 566–578.

O'Connor, B.L., Hondzo, M., Harvey, J.W., 2009. Incorporating both physical and kinetic limitations in quantifying dissolved oxygen flux to aquatic sediments. Journal of Environmental Engineering 135, 1304–1314.

Okumura, M., Fujinaga, K., Seike, Y., HAYASHI, K., 1998. A simple in situ preconcentration method for phosphate phosphorus in environmental waters by column solid phase extraction using activated carbon loaded with zirconium. Analytical sciences 14, 417–419.

Paraska, D.W., Hipsey, M.R., Salmon, S.U., 2014. Sediment diagenesis models: Review of approaches, challenges and opportunities. Environmental Modelling & Software 61, 297–325. https://doi.org/10.1016/j.envsoft.2014.05.011

Phillips, G., 2008. Eutrophication of Shallow Temperate Lakes, in: The Lakes Handbook, Volume 2: Lake Restoration and Rehabilitation. John Wiley & Sons, p. 261.

Santschi, P., Höhener, P., Benoit, G., Buchholtz-ten Brink, M., 1990. Chemical processes at the sediment-water interface. Marine Chemistry 30, 269–315.

Seitaj, D., Sulu-Gambari, F., Burdorf, L.D.W., Romero-Ramirez, A., Maire, O., Malkin, S.Y., Slomp, C.P., Meysman, F.J.R., 2017. Sedimentary oxygen dynamics in a seasonally hypoxic basin. Limnology and Oceanography 62, 452–473. https://doi.org/10.1002/lno.10434

Shaw, D.A., Hanratty, T.J., 1977. Turbulent mass transfer rates to a wall for large Schmidt numbers. AIChE Journal 23, 28–37.

Søndergaard, M., Jensen, J.P., Jeppesen, E., 2003. Role of sediment and internal loading of phosphorus in shallow lakes. Hydrobiologia 506, 135–145.

Sulpis, O., Mucci, A., Boudreau, B.P., Barry, M.A., Johnson, B.D., 2019. Controlling the diffusive boundary layer thickness above the sediment–water interface in a thermostated rotating-disk reactor. Limnology and Oceanography: Methods 17, 241–253. https://doi.org/10.1002/lom3.10309

Sun, X., Humborg, C., Mörth, C.-M., Brüchert, V., 2021. The Importance of Benthic Nutrient Fluxes in Supporting Primary Production in the Laptev and East Siberian Shelf Seas. Global Biogeochemical Cycles 35, e2020GB006849. https://doi.org/10.1029/2020GB006849

Telliard, W., 1997. Determination of trace elements in water by preconcentration and inductively coupled plasma-mass spectrometry. US: Environmental Protection Agency.

Tengberg, A., Hall, P.O.J., Andersson, U., Lindén, B., Styrenius, O., Boland, G., De Bovee, F., Carlsson, B., Ceradini, S., Devol, A., 2005. Intercalibration of benthic flux chambers: II. Hydrodynamic characterization and flux comparisons of 14 different designs. Marine Chemistry 94, 147–173.

Thibodeaux, L.J., Justin, E., Birdwell, J.E., Reible, D.D., 2011. Diffusive Chemical Transport across Water and Sediment Boundary Layers, w: Handbook of Chemical Mass Transport in the Environment. Thibodeaux LJ, Mackay D.(red.), Taylor.

Viollier, E., Rabouille, C., Apitz, S.E., Breuer, E., Chaillou, G., Dedieu, K., Furukawa, Y., Grenz, C., Hall, P., Janssen, F., 2003. Benthic biogeochemistry: state of the art technologies and guidelines for the future of in situ survey. Journal of Experimental Marine Biology and Ecology 285, 5–31.

Wang, W., Wang, W.-X., 2017. Trace metal behavior in sediments of Jiulong River Estuary and implication for benthic exchange fluxes. Environmental Pollution 225, 598–609. https://doi.org/10.1016/j.envpol.2017.03.028

Weber, R.O., 1999. Remarks on the Definition and Estimation of Friction Velocity. Boundary-Layer Meteorology 93, 197–209. https://doi.org/10.1023/A:1002043826623

Wilczak, J.M., Oncley, S.P., Stage, S.A., 2001. Sonic anemometer tilt correction algorithms. Boundary-layer meteorology 99, 127–150.

Woodruff, S., House, W., Callow, M., Leadbeater, B., 1999. The effects of biofilms on chemical processes in surficial sediments. Freshwater Biology 41, 73–89.

Yamamoto, S., Kayanne, H., Tokoro, T., Kuwae, T., Watanabe, A., 2015. Total alkalinity flux in coral reefs estimated from eddy covariance and sediment pore-water profiles. Limnology and Oceanography 60, 229–241. https://doi.org/10.1002/lno.10018

Zhang, H., Davison, W., 1999. Diffusional characteristics of hydrogels used in DGT and DET techniques. Analytica Chimica Acta 398, 329–340.

Supplementary Material

S.1. Flux quality analysis for REA and AEC

Both REA and AEC require fully developed and homogeneous turbulence. As a first criterion, the development of turbulence was assessed by observing the presence of an inertial subrange of slope -5/3 in the power spectral density function of the vertical velocity (Kaimal et al., 1972) during both prototype alignment and flux-averaging periods. For REA only, two additional criteria were considered: the average vertical velocity during a flux-averaging period ($\overline{w}$), ideally zero, should not be larger than the velocity threshold (w_0); and the solute concentration difference between accumulated samples ($\overline{C_\uparrow} - \overline{C_\downarrow}$) should remain above the analytical accuracy of the average concentration. If these criteria are unfulfilled, confidence in the flux value is low, as indicated on Fig. 3.

The time required for aligning REA coordinate system with the vertical was unknown; it was evaluated by computing AEC oxygen fluxes for different durations. Such an approach is relevant since both techniques are based on similar velocity processing and measurement principles and it is only feasible during AEC post-processing, contrary to REA pre-processing. Different prototype alignment periods were tested, from 1 to 12 h before the start of the first flux-averaging period, with 20 min intervals. The angles obtained by planar fit for each duration were applied to the AEC dataset and oxygen fluxes were computed. They were compared with those calculated with the usual AEC processing (see section 2.1), by computing their coefficient of determination and their mean absolute error. A period of 11 h shows a correlation with $R^2 > 0.75$ and a normalized minimum error lower than 10%. Thus, we consider a prototype alignment period of 12 h to be both effective and practical.

S.2. Estimation of flux uncertainty

The errors were propagated to compute the REA and MTC flux uncertainties. The flux equations (Eq. 2 and Eq. 4 and 5) both consist of the product of a prefactor, variables and a concentration difference. The REA flux uncertainty, $u(F_{REA})$, was estimated as:

$$u(F_{REA}) = \sqrt{\left(\frac{u(b)}{b}\right)^2 {F_{REA}}^2 + (b\sigma_w)^2(u(C_\uparrow)^2 + u(C_\downarrow)^2)} \qquad \text{(Eq. S1)}$$

where $u(x)$ is the uncertainty of variable x, neglecting the uncertainty on the standard deviation of velocity due to the high number of points during 20-min flux-averaging periods. Analytical accuracy was used as uncertainty for concentrations. For the coefficient b, Lemaire et al. (2017) gave an interquartile range of 0.4 at zero velocity threshold for oxygen. Assuming a normal distribution, this corresponds to a standard deviation of 0.17 that was used as the uncertainty $u(b)$ after assuming flux similarity between solutes.

MTC flux uncertainty, $u(F_{MTC})$, was estimated by error propagation as:

$$u(F_{MTC}) = \sqrt{\left(\frac{u(u_*)}{u_*}\right)^2 {F_{MTC}}^2 + K^2(u(C_{TBL})^2 + u(C_{SWI})^2)} \quad \text{(Eq. S2)}$$

choosing the standard deviations of: the time series of friction velocity for $u(u_*)$, the temporal replicates for $u(C_{TBL})$, and the spatial replicates for $u(C_{SWI})$.

Meanwhile, both AEC and Sediment Incubation flux uncertainties were equal to their standard deviation of measurements (12 flux-averaging periods and triplicates of miniprofiles, respectively).

S.3. Considerations on spatiotemporal scales

In order to assess the performance of REA and MTC techniques for measuring benthic fluxes *in situ*, we compared their flux values with AEC oxygen fluxes and with reference fluxes by sediment incubation. However, REA and MTC work at different spatiotemporal scales, as illustrated in Figure 1. As for the vertical spatial-scale, sampling height is relevant in terms of mixing rates. We refer to Wüest and Lorke (2003) for definitions of the benthic layers mentioned below. MTC technique requires a measured concentration right at the SWI, *i.e.,* at the DBL's lowest boundary (submillimetre scale). Current speed – for both REA and MTC - was measured above the viscous sublayer (centimetre scale), within the TBL (metre scale). It is done at high frequency (8 Hz) to resolve the turbulent parameters required for REA (w', σ_w, w_0) and MTC (u_*). Water is sampled at high frequency for REA (to accumulate $\overline{C_\uparrow}$ and $\overline{C_\downarrow}$) and once - or averaged from several samples taken during gel exposition - for MTC (C_{TBL}). Regarding the horizontal scale, fluxes measured by the REA (and AEC) are representative for a relatively large sediment surface (~200 m^2), as compared with other methods. This is defined by its footprint size, *i.e.,* the area of the sediment contributing to measured fluxes (Berg et al., 2007; Foken and Napo, 2008; Kljun et al., 2015). This is an advantage of the method because it avoids the simultaneous use of several measuring systems as for MTC (also for micro-profiles or benthic chambers) in spatially heterogeneous environments. Finally, regarding the time scales of the resulting benthic fluxes, REA (and AEC) fluxes are representative for 20-30 min according to its flux-averaging periods (a similar time is required in between flux-averaging periods for collecting and filtering the samples plus setting the instrument for new measurements), while MTC (and sediment incubations) of 6-8 h according to gel exposition. All these technical differences have to be taken into account when comparing the resulting fluxes.

S.4. Study site

Lake Champs-sur-Marne is a small, shallow, urban lake located in the east of Paris, France (Fig. S4). Originally formed as a sandpit and now used for recreational purposes, it has a surface area of 0.12 km^2, a mean depth of 2.5 m, and a maximum depth of 3.5 m (Piccioni et al., 2021). It is hyper-eutrophic with recurrent algal blooms, and its proximity to the Marne River (~100 m away) explains that its water quality is affected by the river's water quality. However, the only connection to the river is via groundwater flow, as the lake has no surface inflow or outflow.

Measurements were performed from a boat in the southeast part of the lake (Fig. S4) where the water depth is 3.3 m. This location was selected because of the presence of muddy sediments with high microbial activity, but without macrophytes. Measurements were performed on June 13, 2021.

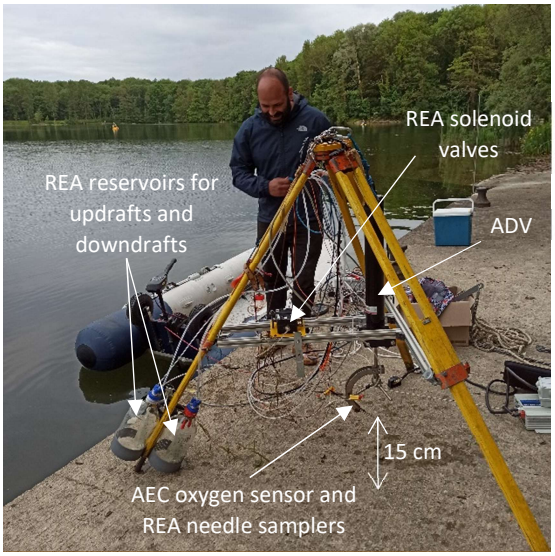

Figure S1. Deploying frame used for Relaxed Eddy Accumulation (REA) and Aquatic Eddy Covariance (AEC) systems. Acoustic Doppler Velocimeter (ADV) is used for both systems. Technical details on REA and AEC systems in Calabro-Souza et al. (2023).

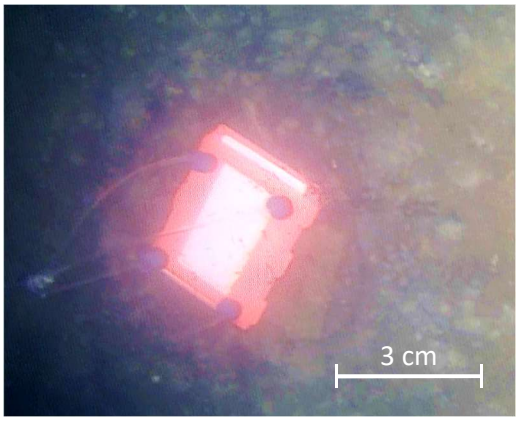

Figure S2. Interface peeper lying on the sediment surface at 3 m depth in Lake Champs.

Figure S3. Side-looking ADV positioning frame used for the Mass Transfer Coefficient (MTC) method

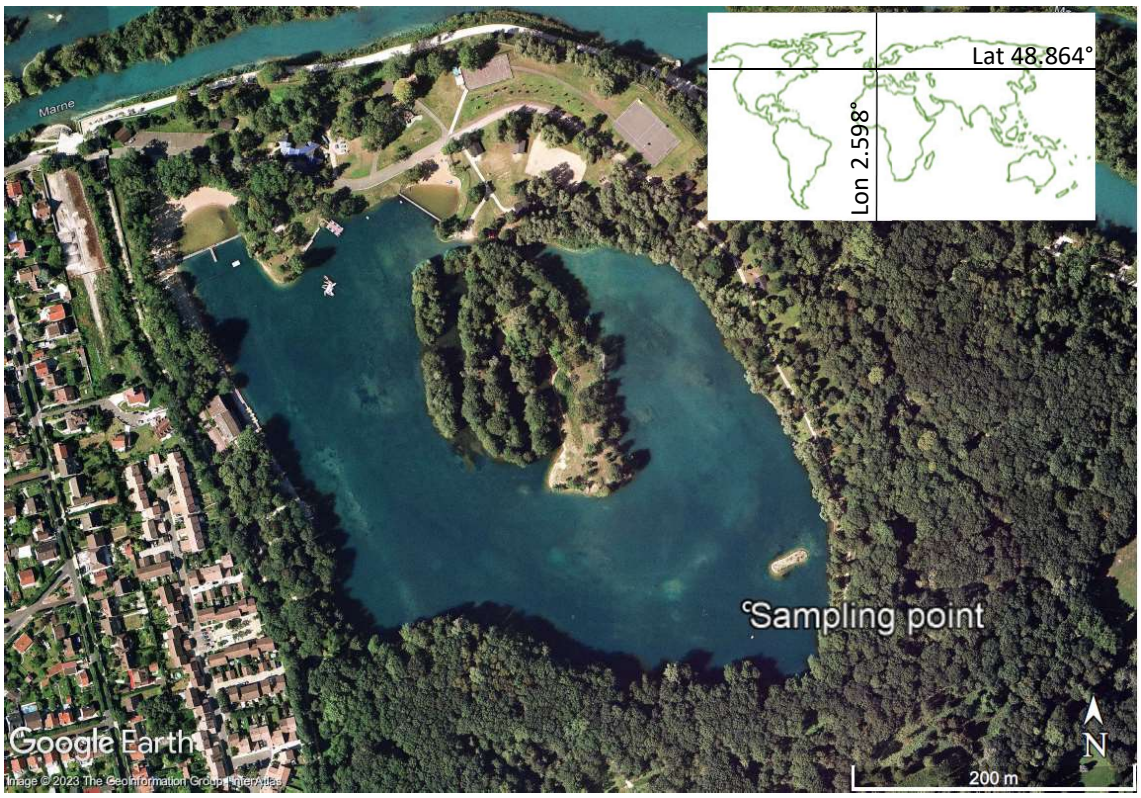

Figure S4 - Lake Champs-sur-Marne is a shallow urban lake that shows significant primary production during summer. It is located in East Paris, France, next to the Marne River. The sampling point (shown) was selected within the deepest zone of the lake (3 m) with muddy sediments and absence of macrophytes (source: Google Earth).

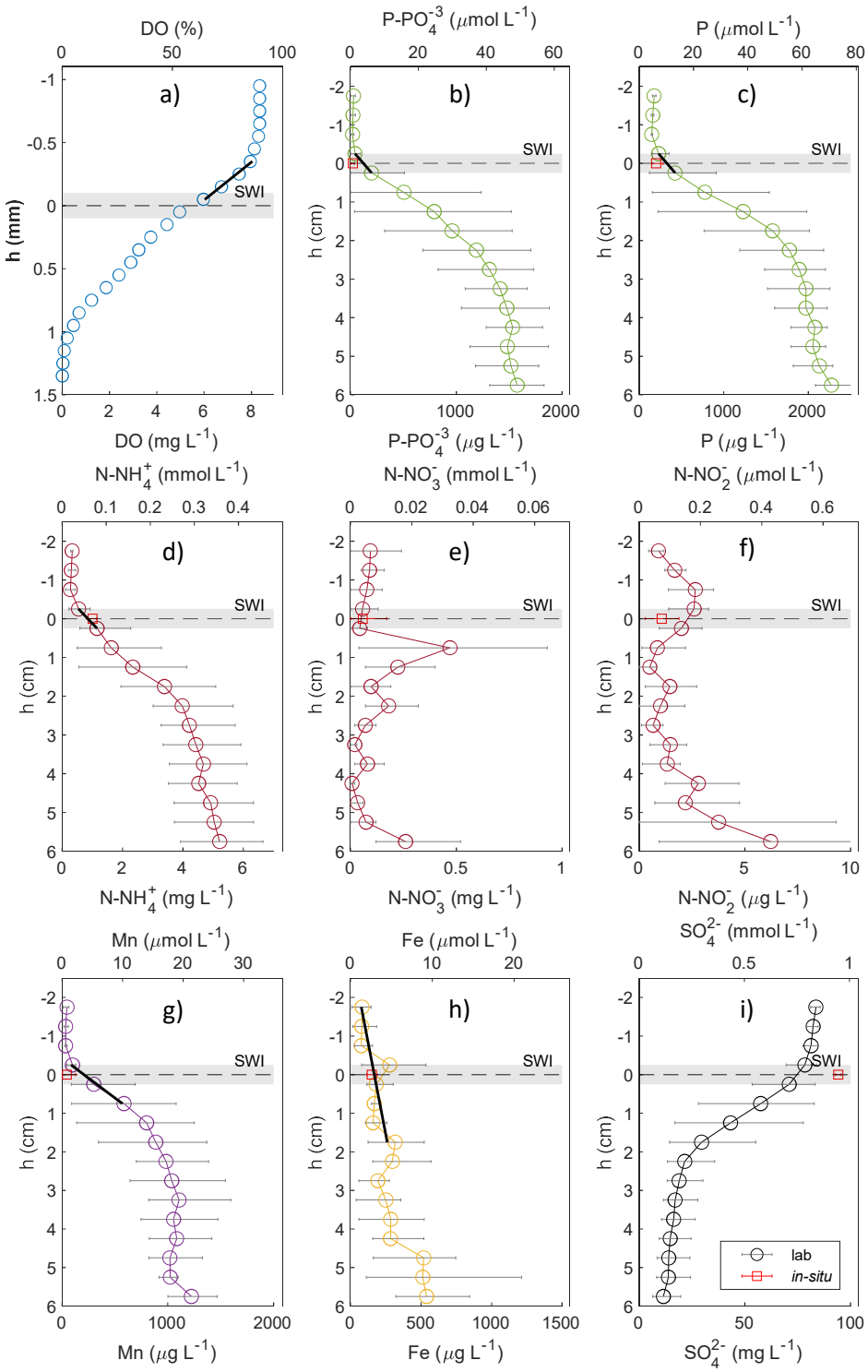

Figure S5 - Concentration profiles of chemicals dissolved in porewater and overlying water from sediment core incubation (lab) and field measurements (in situ). Upper-left panel a): Dissolved Oxygen (DO) measured with a micro-optode. Other panels include b) phosphate phosphorus, c) total phosphorus, d) ammonium, e) nitrate and f) nitrite nitrogen, g) manganese, h) iron, and i) sulphate, all sampled by minipeepers (Diffusive Equilibrium in Thin-films, DET). Circles correspond to the average concentrations of three minipeepers deployed in each of the three sediment cores. Horizontal bars represent their respective maximum and minimum values. Concentrations at the SWI measured from interface peepers are shown as red squares. Thick black lines show interfacial gradient used for flux estimation. Porewater profiles of (total) phosphorus, nitrate, nitrite, and sulphate are also provided for a better description of sediment biogeochemistry. The sediment-water interface (SWI) is located at depth (h) equal to zero (horizontal dashed line). The uncertainty on its visual detection is around 0.1 and 2.5 mm for oxygen and other profiles, respectively (grey shaded area).

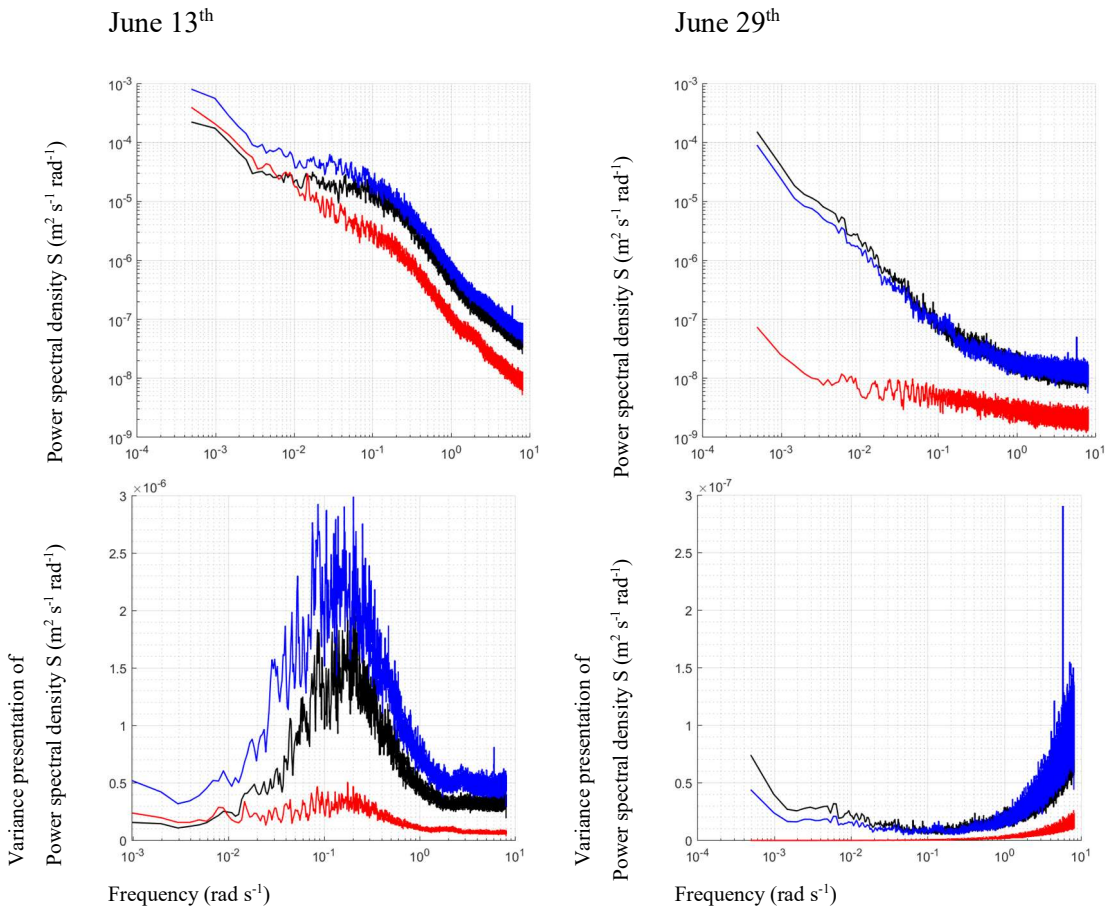

Figure S6. Example of power spectra showing turbulence presence (left) and absence (right) for longitudinal (black), lateral (blue), and vertical (red) velocity components. Measurements from June 13th show a turbulent inertial subrange that withstands for frequencies higher than 0.3 Hz, which is not the case for June 29th.

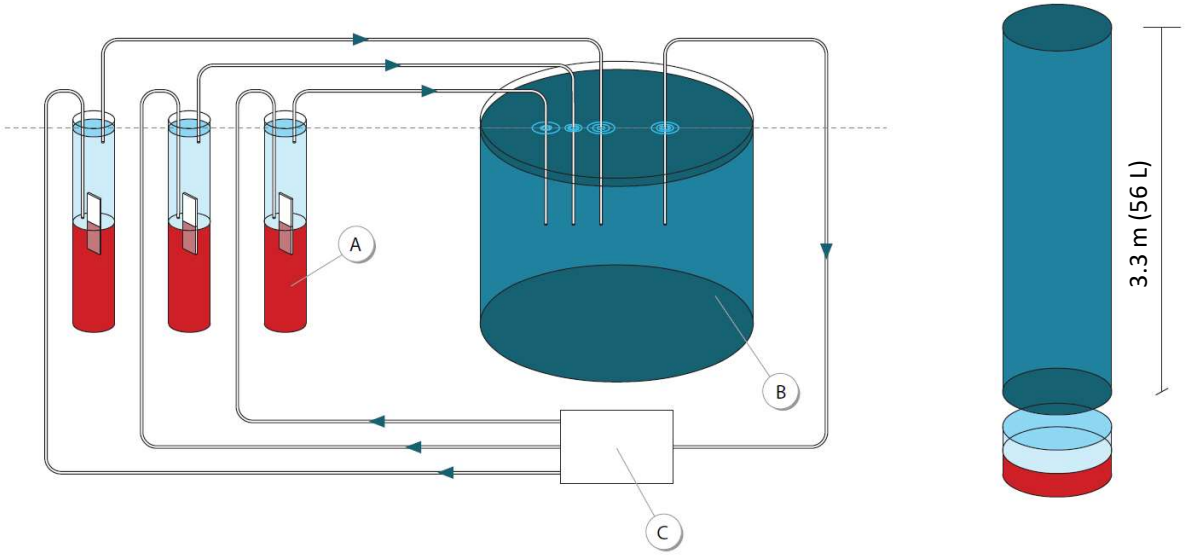

Figure S7. Lab incubation diagram of sediment cores (left). Three sediment cores were incubated with a recirculating volume of water equivalent to its respective water column (right). Fluxes were estimated by applying Fick's law to interfacial concentration gradients that were detected with gel minipeepers. Letters in diagram correspond to: (A) sediment core, (B) reservoir for lake water (56 L), and (C) pump and valves system.

Table S1 - The main difficulty of REA is to measure small relative concentration differences. Upward (C_{up}) and downward (C_{down}) concentrations from accumulated water samples collected by Relaxed Eddy Accumulation (REA). Concentration difference ($\Delta C = C_{up} - D_{down}$) expressed as absolute and percentage values

C (mmol m^{-3})		**10:51**	**11:30**	**12:05**	**12:47**	**13:57**	**14:47**	**15:33**	**16:28**	**17:10**
NH_4^+	**C_{up}**	1.80	1.89	2.24	1.98	1.62	1.80	1.89	1.80	1.62
	C_{down}	2.24	1.98	1.71	1.89	1.53	1.53	1.62	1.89	1.62
	ΔC	-0.44	-0.09	0.53	0.09	0.09	0.27	0.27	-0.09	0.00
	ΔC (%)	22	5	27	5	6	16	15	5	0
PO_4^{3-}	**C_{up}**	6.7	6.8	6.7	6.7	6.7	7.0	6.9	6.7	6.7
	C_{down}	6.7	6.7	6.7	6.6	6.4	6.9	6.7	6.7	6.7
	ΔC	-0.01	0.06	0.08	0.08	0.30	0.08	0.14	0.06	0.00
	ΔC (%)	0.2	0.9	1.2	1.2	4.6	1.1	2.1	0.8	0.0
Fe	**C_{up}**	0.056	0.023	0.039	0.062	0.041	0.066	0.041	0.049	0.042
	C_{down}	0.069	0.036	0.034	0.040	0.036	0.039	0.038	0.044	0.035
	ΔC	-0.01	-0.01	0.01	0.02	0.01	0.03	0.00	0.01	0.01
	ΔC (%)	21	43	14	42	13	50	9	12	17
Mn	**C_{up}**	0.054	0.022	0.050	0.070	0.039	0.083	0.056	0.059	0.043
	C_{down}	0.059	0.041	0.041	0.051	0.039	0.041	0.039	0.047	0.059
	ΔC	-0.01	-0.02	0.01	0.02	0.00	0.04	0.02	0.01	-0.02
	ΔC (%)	10	61	21	32	0	68	35	23	32

Table S2 - Benthic fluxes estimated by applying Fix's law to interface gradients obtained from sediment incubations. Errors expressed as standard deviations.

Compound	Ion diffusivity (10^{-9} m^2 s^{-1})	dC/dz (mg L^{-1} cm^{-1})	Flux in incubation cores (mmol m^{-2} day^{-1})
Oxygen	2.01	-67 ± 20.1	-36.4 ± 10.9
Ammonium	1.73	1.23 ± 0.78	1.31 ± 0.83
Phosphate	0.79	0.31 ± 0.1	0.07 ± 0.02
Iron	1.04	0.05 ± 0.02	0.01 ± 0
Manganese	1.05	0.49 ± 0.36	0.08 ± 0.06

Table S3 - Benthic fluxes measured in Lake Champs by Relaxed Eddy Accumulation (REA), Mass Transfer Coefficient (MTC), Sediment Incubation, and Eddy Covariance (AEC)

Fluxes (mmol m^{-2} d^{-1})					
	Oxygen	**Ammonium**	**Phosphate**	**Manganese**	**Iron**
REA	-	23.5 ± 8.8	7.7 ± 12.1	1 ± 1.3	0.8 ± 1.1
MTC	-	42.2 ± 25.7	0.2 ± 0.3	0.8 ± 1.5	0.7 ± 1
Sed. Inc.	-36.4 ± 10.9	1.31 ± 0.83	0.07 ± 0.02	0.01 ± 0	0.08 ± 0.06
AEC	-14.6 ± 4.3	-	-	-	-

Table S4 – Reference values of benthic fluxes found in literature

Reference Paper	Waterbody type	Technique	Substance	Flux (mmol m^{-2} d^{-1})
Forja and Gómez-Parra, 1998	Bay of Cadiz (Spain)	Benthic chambers	Ammonia	20
			Phosphate	6
		Sediment Core	Ammonia	3
			Phosphate	0.5
Grüneberg et al., 2015	River Havel (Germany)	Benthic chambers and peepers	Ammonium	8.9
			Soluble Reactive P	1.1
		Peepers	Soluble Reactive P	0.2
			Ammonium	1.6
Callender and Hammond, 1982	Potomac river (USA)	Benthic chambers	Ammonium	26
			Phosphate	4
Reay et al., 1995	Chesapeake Bay (USA)	Benthic chambers	Ammonium	13.9
Human et al., 2020	Knysna Estuary (RSA)	Benthic chambers	Ammonium	72
			Soluble Reactive P	8.4
Kim et al., 2021	Aquaculture (South Korea)	Benthic chambers	Ammonium	16.2
			Phosphate	2.5
Shim et al., 1997	Aquaculture (South Korea)	Benthic chamber	Phosphate	2.5
			Ammonium	15.7

References

Berg, P., Røy, H., Wiberg, P.L., 2007. Eddy correlation flux measurements: The sediment surface area that contributes to the flux. Limnology and Oceanography 52, 1672–1684.

Calabro-Souza, G., Lorke, A., Noss, C., Dubois, P., Saad, M., Ramos-Sanchez, C., Vinçon-Leite, B., Moilleron, R., Jodeau, M., Lemaire, B.J., 2023. A New Technique for Resolving Benthic Solute Fluxes: Evaluation of Conditional Sampling Using Aquatic Relaxed Eddy Accumulation. Earth and Space Science 10, e2023EA003041. https://doi.org/10.1029/2023EA003041

Callender, E., Hammond, D.E., 1982. Nutrient exchange across the sediment-water interface in the Potomac River estuary. Estuarine, Coastal and Shelf Science 15, 395–413.

Foken, T., Napo, C.J., 2008. Micrometeorology. Springer.

Forja, J.M., Gómez-Parra, A., 1998. Measuring nutrient fluxes across the sediment-water interface using benthic chambers. Marine Ecology Progress Series 164, 95–105.

Grüneberg, B., Dadi, T., Lindim, C., Fischer, H., 2015. Effects of nitrogen and phosphorus load reduction on benthic phosphorus release in a riverine lake. Biogeochemistry 123, 185–202. https://doi.org/10.1007/s10533-014-0062-3

Human, L., Weitz, R., Allanson, B., Adams, J., 2020. Nutrient fluxes from sediments pose management challenges for the Knysna Estuary, South Africa. African Journal of Aquatic Science 45, 1–9. https://doi.org/10.2989/16085914.2019.1671787

Kaimal, J.C., Wyngaard, J., Izumi, Y., Coté, O., 1972. Spectral characteristics of surface-layer turbulence. Quarterly Journal of the Royal Meteorological Society 98, 563–589.

Kim, S.-H., Lee, J.-S., Kim, K.-T., Kim, H.-C., Lee, W.-C., Choi, D., Choi, S.-H., Choi, J.-H., Lee, H.-J., Shin, J.-H., 2021. Aquaculture Farming Effect on Benthic Respiration and Nutrient Flux in Semi-Enclosed Coastal Waters of Korea. Journal of Marine Science and Engineering 9, 554. https://doi.org/10.3390/jmse9050554

Kljun, N., Calanca, P., Rotach, M.W., Schmid, H.P., 2015. A simple two-dimensional parameterisation for Flux Footprint Prediction (FFP). Geoscientific Model Development 8, 3695–3713. https://doi.org/10.5194/gmd-8-3695-2015

Lemaire, B.J., Noss, C., Lorke, A., 2017. Toward relaxed eddy accumulation measurements of sediment-water exchange in aquatic ecosystems. Geophysical Research Letters 44, 8901–8909. https://doi.org/10.1002/2017gl074625

Piccioni, F., Casenave, C., Lemaire, B.J., Le Moigne, P., Dubois, P., Vinçon-Leite, B., 2021. The thermal response of small and shallow lakes to climate change: new insights from 3D hindcast modelling. Earth System Dynamics 12, 439–456. https://doi.org/10.5194/esd-12-439-2021

Reay, W.G., Gallagher, D.L., Simmons, G.M., 1995. Sediment-water column oxygen and nutrient fluxes in nearshore environments of the lower Delmarva Peninsula, USA. Marine Ecology Progress Series 118, 215–227.

Shim, J.-H., Kang, Y.-C., Choi, J.-W., 1997. Chemical fluxes at the sediment-water interface below marine fish cages on the coastal waters off Tong-Young, south coast of Korea. The Sea: JOURNAL OF THE KOREAN SOCIETY OF OCEANOGRAPHY 2, 151–159.

Wüest, A., Lorke, A., 2003. Small-Scalehydrodynamics Inlakes. Annual Review of Fluid Mechanics 35, 373–412. https://doi.org/10.1146/annurev.fluid.35.101101.161220